Toxicity and photosensitizing assessment of gelatin methacryloyl-based hydrogels photoinitiated with lithium phenyl-2,4,6-trimethylbenzoylphosphinate in human primary renal proximal tubule epithelial cells

Alexander K. Nguyen,[1,2] Peter L. Goering,[2,a)] Vytas Reipa,[3] and Roger J. Narayan[1,a)]
[1]*UNC/NCSU Joint Department of Biomedical Engineering, North Carolina State University, Campus Box 7115, 911 Oval Drive, Raleigh, North Carolina 27695*
[2]*Division of Biology, Chemistry, and Materials Science, US Food and Drug Administration, 10903 New Hampshire Ave., Silver Spring, Maryland 20993*
[3]*Biosystems and Biomaterials Division, National Institute for Standards and Technology, 100 Bureau Drive, Gaithersburg, Maryland 20899*

(Received 13 March 2019; accepted 17 April 2019; published 3 May 2019)

Gelatin methacryloyl (GelMA) and lithium phenyl-2,4,6-trimethylbenzoylphosphinate (LAP) photoinitiator are commonly used in combination to produce a photosensitive polymer but there are concerns that must be addressed: the presence of unreacted monomer is well known to be cytotoxic, and lithium salts are known to cause acute kidney injury. In this study, acellular 10% GelMA hydrogels cross-linked with different LAP concentrations and cross-linking illumination times were evaluated for their cytotoxicity, photosensitizing potential, and elastic moduli. Alamar Blue and CyQuant Direct Cell viability assays were performed on human primary renal proximal tubule epithelial cells (hRPTECs) exposed to extracts of each formulation. UV exposure during cross-linking was not found to affect extract cytotoxicity in either assay. LAP concentration did not affect extract cytotoxicity as determined by the Alamar Blue assay but reduced hRPTEC viability in the CyQuant Direct cell assay. Photocatalytic activity of formulation extracts toward NADH oxidation was used as a screening method for photosensitizing potential; longer UV exposure durations yielded extracts with less photocatalytic activity. Finally, elastic moduli determined using nanoindentation was found to plateau to approximately 20–25 kPa after exposure to 342 mJ/cm^2 at 2.87 mW of UV-A exposure regardless of LAP concentration. LAP at concentrations commonly used in bioprinting (<0.5% w/w) was not found to be cytotoxic although the differences in cytotoxicity evaluation determined from the two viability assays imply cell membrane damage and should be investigated further. Complete cross-linking of all formulations decreased photocatalytic activity while maintaining predictable final elastic moduli. *Published by the AVS.* https://doi.org/10.1116/1.5095886

I. INTRODUCTION

Precise control of device geometry and mechanical properties in tissue engineering constructs is required to recapitulate stem cell behavior as to elicit the intended cellular response. Many additive manufacturing materials and methods are detrimental to cell viability due to extreme conditions such as heat, pressure, and/or chemical toxicity. Novel developments in photosensitive polymers bridge this gap by avoiding excessive heat and pressure, such as those found in fused deposition modeling, while reducing the impact of chemical toxicity. Photosensitive, cell-laden tissue engineering constructs have been fabricated using methods including bulk polymerization[1] and micromolding.[2] Beyond the direct injection or casting of the liquid cell-laden photopolymer for implantation, additive manufacturing using stereolithography[3,4] or especially extrusion bioprinting[5–7] of these gels is a popular method to impart needed features such as pores for nutrient exchange.

There are two general strategies to bioprinted constructs: fabrication of an acellular scaffold followed by seeding with cells or direct fabrication of the constructs with cells *in situ*. Both methods come with their own benefits and drawbacks but share many common challenges. In either case, the base polymer and photoinitiator have highly reactive chemical moieties that allow them to participate in the cross-linking reaction. The base materials and their reaction by-products can be materials of toxicological concern especially with polymerization with cells *in situ*. In this case, there would be no postprocessing step that would allow these potentially toxic materials to leach out before exposure to cells or tissue. The second concern unique to photosensitive polymers is potential adverse responses resulting from photosensitization; cells seeded in the presence of UV and/or visible light dyes could be at greater risk to phototoxicity. This possibility is compounded further in the direct fabrication of cell constructs due to the exposure of the cells to UV and/or visible radiation. Finally, this photopolymer system must retain practical polymerization rates and mechanical properties to be a workable candidate for bioprinting.

[a)]Authors to whom correspondence should be addressed: Peter.Goering@fda.hhs.gov and rjnaraya@ncsu.edu

Photopolymers are composed of a base monomer or oligomer combined with a photoinitiator. This type of polymer is commonly a simple mixture of the two compounds although it is possible to integrate the photoinitiator into the polymer itself.[8] Popular reactive moieties include epoxy,[9] thiol-ene,[10–12] and acrylate chemistries and are matched with a compatible photoinitiator chemistry. For example, SU-8 is a popular biocompatible polymer designed for the microelectronics industry but has found uses in biomedical research; this polymer uses epoxy ring-opening chemistries combined with a photoacid generator. However, the most popular reactive group in bioprinting is the acrylate group which undergoes radical chain polymerization and can be photoinitiated by free radical-generating photoinitiators.

Gelatin methacryloyl (GelMA) contains acrylate groups on a gelatin backbone and can therefore be cross-linked in the presence of free-radical photoinitiators for use in bioprinting. It is also one of the most popular, commercially-available photosensitive hydrogels for bioprinting because of its facile synthesis methods, tunability of mechanical properties, and cytocompatibility.[13,14] This material is normally used with Irgacure 2959, which provides such advantages as water-solubility and acceptable cytotoxicity.[15,16] Even so, Irgacure 2959 is not ideal for use because it has peak absorption at 280 nm with tail absorption in the UV-A spectrum. In addition, UV-B light emitting diodes (LEDs) are much more expensive, have shorter life spans versus UV-A LEDs, and have a greater potential to produce genotoxic effects;[17] use of UV-A or visible light for cross-linking is preferred for these reasons. Lithium phenyl-2,4,6-trimethylbenzoylphosphinate (LAP) is an alternative photoinitiator that is more water soluble than Irgacure 2959 and has peak absorption in the UV-A spectrum and tail absorption in the visible spectrum. Direct comparison of Irgacure 2959 and LAP as photoinitiators for polyethyleneglycol diacrylate as a model acrylate hydrogel revealed gelation times 10× faster with LAP versus Irgacure 2959 using 365 nm light at similar concentrations and UV-A exposures.[18] Exposure of PEGda gels with LAP to 405 nm light was also faster than the corresponding Irgacure 2959 gel exposed to 365 nm light with a gelation time of 120 s vs 212 s, respectively.

Due to its promise as a photopolymer formulation for bioprinting, GelMA with LAP should be closely evaluated for its compatibility with cells and tissue. LAP is a lithium salt and would expose incorporated cells and surrounding tissues to lithium ions. Ionic lithium is a treatment for bipolar disorder with a narrow therapeutic blood serum concentration between 0.4 and 0.75 mmol/l with excursions to as much as 1.2 mmol/l.[19] Serum lithium of 1.4 mmol/l is the lower threshold of acute toxicity while concentrations exceeding 3.5 mmol/l are considered toxic to patients. The main adverse effects are neurological; however, renal tubulointerstitial nephropathy and nephrogenic diabetes insipidus have been noted.[20] A small hydrogel implant would not raise blood serum levels to these thresholds which makes adverse neurological effects unlikely, but local concentrations of lithium range from 1.7 mmol/l for gels containing 0.05% w/w LAP to 34 mmol/l for 1% LAP gels, which is of potential concern to the embedded cells and surrounding tissue. Although lithium has been shown to cause diabetes insipidus by affecting membrane localization of aquaporin-2 in kidney nephron collecting duct cells,[21] acute tubulointerstitial nephropathy caused by proximal tubule cell damage can cause irreversible reduction in kidney function.[22] Therefore, the goal of this study was to evaluate toxicity in human renal proximal tubule endothelial cells (hRPTECs) that were acutely exposed to different formulations of GelMA hydrogel extracts using various LAP concentrations and UV-A exposures used during cross-linking to model proximal tubule tissue in close proximity to a GelMA-LAP hydrogel implant.

II. EXPERIMENT

A. UV-vis spectrometry of LAP and Irgacure 2959

Solutions (0.1% w/w) of LAP and Irgacure 2959 were serially diluted to produce 1, 0.2, 0.04, and 0.008 mg/ml solutions in ultrapure water. Aliquots (200 μl) of each solution were loaded into a UV-transparent, 96-well plate (Greiner Bio-One GmbH, Frickenhausen, Germany) and the absorbance read from 190 to 850 nm on a SpectraMax190 plate reader (Molecular Devices, San Jose, CA). Emission spectra of the fluorescent UV-A light source within the UV curing oven (CL-1000L, Analytik Jena US, Upland, CA), modified with a soda lime glass plate in front of the light source to filter out UV-B wavelengths, were characterized with a spectrometer (Ocean Optics, Largo, FL).

B. Cell culture

hRPTECs (PCS-400-010, lot 63010943, ATCC, Manassas, VA) were received from the manufacturer cryopreserved at passage 2 and cultured using renal epithelial cell basal medium (PCS-400-030) with the renal epithelial cell growth kit (PCS-400-040). hRPTECs were cultured through an additional passage then cryopreserved at passage 4 in media with 10% v/v dimethyl sulfoxide and 15% fetal bovine serum at 3.85×10^6 cells/ml. Each experimental replicate used a passage 4 cryopreserved vial grown through one passage before seeding. Thus, hRPTECs used in the study were at passage 5.

C. 10% w/w GelMA-LAP formulations and extraction

LAP and GelMA were purchased from Allevi (Philadelphia, PA). GelMA used in this study is sourced from type A, 300 bloom gelatin sourced from porcine skin and has a 50% degree of methacrylation. GelMA (10% w/w) was produced by weighing dry GelMA on an analytical balance (M-220, Denver Instrument, Bohemia, NY), adding the appropriate mass of water, then sonicating the mixture for 30 min at 40 °C. LAP was weighed on a six-point balance (XP56, Mettler Toledo, Columbus, OH), the appropriate mass of 10% GelMA added to form a 1% w/w LAP concentration, and the mixture sonicated for 30 min at 40 °C.

Both the plain 10% GelMA solution and the 10% GelMA containing 1% LAP were sterile-filtered through a 0.2 μm PES membrane (Millipore, Burlington, MA). Appropriate volumes of each were mixed to produce 0.1%, 0.25%, 0.5%, and 1% w/w LAP in 10% GelMA and exposed to one of three UV-A exposure durations: 30, 120, or 300 s in a CL-1000L UV cross-linking oven; these exposure times correspond to 86, 342, or 855 mJ/cm^2 of UV-A radiation. Thus, a test matrix composed of four LAP concentrations and three UV-A exposure durations was created for a total of 12 formulations.

GelMA solutions (1 ml) with 0.1%, 0.25%, 0.5%, or 1% w/w LAP were deposited on polystyrene petri-dishes and exposed to 86, 342, or 855 mJ/cm^2 of UV-A according to the experimental design. Gels were removed from the polystyrene using a polytetrafluoroethylene (PTFE) cell scraper and transferred to preweighed 15 ml conical centrifuge tubes and the gel mass measured on an analytical balance. Gels were extracted in cell culture media containing additional penicillin and streptomycin (30-2300, ATCC, Manassas, VA) at a 0.1 g/ml gel mass to media volume ratio for 24 h at 37 °C on a shaker plate. This extraction ratio is suggested for irregularly shaped porous devices by ISO 10993-12:2012.[23] Following extraction, gel extracts were aliquoted and stored at −20 °C until use for the cytotoxicity and photocatalysis assays.

D. Alamar Blue/CyQuant Direct Cell viability assays

Three wells per treatment group were seeded with 1.0×10^4 cells/well and incubated for 24 h before toxicant addition. Media within seeded wells were aspirated and replaced with 100 μl of GelMA formulation extract. Media, or media with 30 μM $AgNO_3$, was added as the negative and positive cytotoxicity controls, respectively; an additional 100 μl of each solution was added to cell-free wells as the assay blank. hRPTECs were exposed to the toxicants for 24 h before addition of 10 μl of Alamar Blue dye. All plates were incubated for 4 h before reading on a fluorescent plate reader at 570 nm emission and 585 nm emission wavelengths. CyQuant dye and background suppression compound were added to the wells after the Alamar Blue data were collected and the plate incubated for an additional 30 min before reading at 480 nm excitation and 535 nm excitation wavelengths. Three independent replicate experiments of the described procedure were performed.

E. NADH photocatalysis assay

Photocatalytic activity of the LAP extracts toward NADH oxidation was measured using UV-A or visible illumination based on a method, described by Lee *et al.*[24] Photogenerated reactive oxygen species (ROS) converts the fluorescent NADH molecule to NAD^+ which is nonfluorescent. A clear-bottomed, black 96-well plate (Sigma Aldrich, St. Louis, MO), containing GelMA-LAP extracts or LAP at several concentrations in triplicate, was filled with a 150 μM NADH (Sigma Aldrich, St. Louis, MO) solution in phosphate-buffered saline (PBS). The plate was exposed to either UV-A light at 5.5 mW/cm^2 by placing it on a transilluminator (Model 2UV, UVP Inc., Upland, CA) or visible light at 7 mW/cm^2; light from a 300 W Xenon arc lamp (Oriel Instruments, Stratford, CT) was filtered through a 1 in. thick quartz flask filled with water to filter out infrared wavelengths, and a 400 nm longpass filter (10LWF-400-B, Oriel Instruments, Stratford, CT). A fluorescence reading at 340 nm excitation and 460 nm emission wavelengths was recorded every minute. The NADH oxidation rate is calculated from the linear portion of the NADH fluorescence decay curve.

F. GelMA chips for assessment of elastic moduli by nanoindentation testing

GelMA chips (12 mm diameter, 1 mm thick) of each formulation were polymerized on 3-(trimethoxysilyl)propylmethacrylate (MAPTMS, Sigma Aldrich, St. Louis, MO) functionalized glass slides. In brief, glass microscope slides were etched with 2.8M NaOH at 60 °C, rinsed in de-ionized water, then sonicated in toluene containing 3% v/v MAPTMS for 30 min. Silanized slides were rinsed in toluene then heated at 150 °C for 1 h under vacuum. MAPTMS-functionalized slides were stored under vacuum until use.

PTFE molds containing a 12 mm diameter × 1 mm deep cavity were used for GelMA chip polymerization. For each gel formulation, molds were filled with the corresponding GelMA-LAP solution, capped with an MAPTMS-functionalized slide, then exposed to UV-A for the prescribed duration. The PTFE molds were removed and the glass slides with attached GelMA chips stored in PBS at 4 °C.

GelMA chips of each formulation underwent nanoindentation testing through the Bio Hardness Tester (Anton Paar, Graz, Austria) with a 500 μm radius spherical ruby tip, and the testing was performed at 23 °C in ambient air condition. Loading/unloading cycles consisted of a 1.2 milliNewton per minute (mN/min) loading rate to a maximum of 0.2 mN, a 30 s pause maintaining 0.2 mN force, followed by a 1.2 mN/min unloading rate to 0 mN. Elastic moduli (E_{IT}) were calculated using the Hertz solution for spherical contact assuming a 0.5 Poisson's ratio and that the reduced modulus is equal to E_{IT} due to the indenter modulus being much greater than the gel modulus. E_{IT} was calculated using the formula[25]

$$P = \frac{4}{3} E_{IT} \sqrt{rh^3},$$

where P is the indentation load, r is the indenter tip radius, and h is the indentation depth. Seven measurements at different locations on the surfaces were performed on a chip representative of each formulation.

G. Statistical analyses

Statistical analysis and graphics generation were performed using Graphpad Prism 6 (La Jolla, CA). Two-way ANOVA was performed on the Alamar Blue and CyQuant

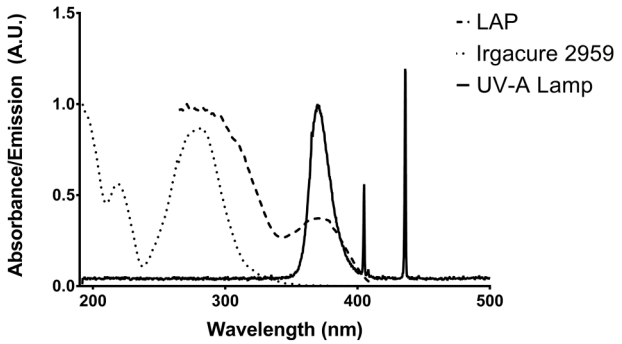

FIG. 1. UV-visible absorption spectra of Irgacure 2959 and LAP in ultrapure water superimposed on the fluorescent UV-A light source emission spectra normalized to the UV-A emission peak. The LAP absorbance peak at 370 nm matches the UV-A emission peak of the fluorescent light source. Irgacure 2959 has tail absorbance in this wavelength range.

Direct Cell datasets with grouping by LAP concentration and UV exposure used in the fabrication of the GelMA chips. Dunnett's multiple comparison *post hoc* test was performed to compare each of the formulations to the negative control. Linear regression was also performed on Alamar Blue and CyQuant Direct Cell datasets after pooling the measurements from the UV exposure treatment groups to display cell viability versus LAP concentration in the photopolymer formulation.

III. RESULTS AND DISCUSSION

A. LAP has peak absorbance in the UV-A spectrum with tail absorbance in the visible spectrum

UV-visible spectra of the fluorescent UV-A source emission, LAP absorbance, and Irgacure 2959 absorbance are presented in Fig. 1. The light source emits sharp 436 nm and 405 nm peaks corresponding to the typical Hg visible emission peaks and a broad peak at 370 nm with a full width at half maximum of 20 nm. LAP exhibits an absorbance peak centered at 370 nm with 14.1% remaining at 405 nm. Irgacure 2959 exhibits peak absorbance at 280 nm and trails off to less than 0.5% of peak absorbance values at 370 nm.

B. Cross-linking duration has no effect on cytotoxicity of GelMA-LAP extracts; LAP concentration is negatively correlated with cell viability in the CyQuant Direct Cell assay

Viability of hRPTEC after 24 h exposure to a GelMA formulation extracts was evaluated using Alamar Blue and CyQuant Direct Cell assays (Fig. 2). Alamar Blue is a resazurin-based assay correlating the generation of highly-fluorescent resorufin resulting from cell metabolism to cell viability. CyQuant Direct Cell Proliferation assay is based on the CyQuant DNA stain but is performed on whole cells instead of cell lysates; the fluorescent stain is membrane-permeable but the background suppression reagent is not; thus, only DNA in live cells with intact membranes will fluoresce. Using viability assays dependent on different mechanisms, i.e., metabolism versus membrane integrity, also gives insight into the mechanism of cytotoxicity.

Neither LAP concentration in the GelMA photopolymer nor UV exposure used during cross-linking was identified as a significant source of variation in hRPTEC viability as judged by the Alamar Blue assay with all formulation extracts resulting in viability not significantly different from the negative control. Viability as judged by the CyQuant Direct Cell assay was not affected by the UV exposure used during cross-linking. Viabilities for the 0.1%, 0.25%, 0.5%, and 1% LAP formulations were 92.5%, 85.4%, 78.9%, and 67.1%, respectively, when averaging results from the three UV exposure scenarios. Viability of hRPTECs exposed to extracts from GelMA formulations containing 1% LAP in all UV exposure scenarios and those from the formulation containing 0.5% LAP exposed to 855 mJ/cm^2 UV-A was statistically different from the negative control. Because UV-A exposure used in cross-linking did not have a significant effect on extract cytotoxicity as determined from ANOVA, measurements from the UV-A exposure treatment groups were pooled for linear regression analysis (Fig. 3). The concentration-response curve for hRPTEC viability as a function of LAP concentration in the GelMA formulation as determined by the Alamar Blue assay did not have a significant nonzero slope while the concentration-response curve as determined by the CyQuant Direct Cell assay revealed

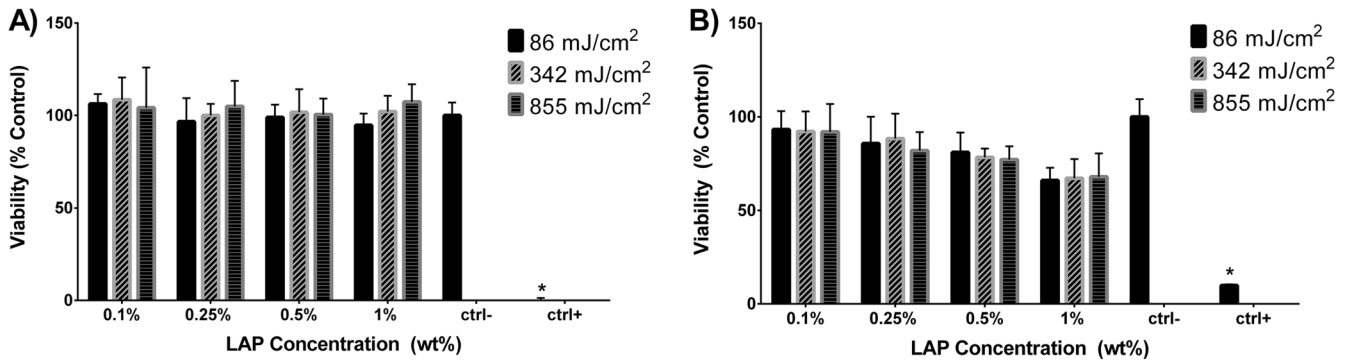

FIG. 2. Viability of hRPTEC exposed for 24 h to GelMA-LAP extracts determined via (a) Alamar Blue and (b) CyQuant Direct Cell assay. Values represent $\bar{X} \pm SD$ of n = 3 independent experimental replicates. Ctrl− = cell media negative control; ctrl+ = 30 μM $AgNO_3$ positive control. Values marked with an asterisk (*) are statistically different from the negative control.

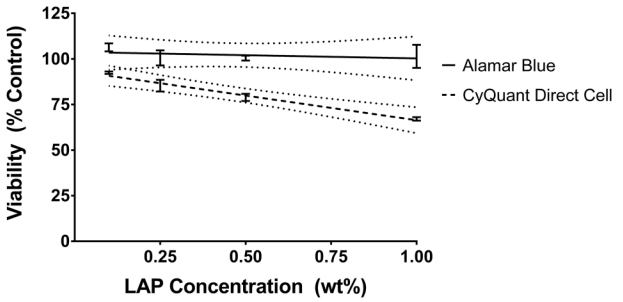

FIG. 3. No effect on hRPTEC viability of LAP concentration in GelMA formulations was determined using the Alamar Blue assay on formulation extracts. Linear regression analysis determined a statistically significant correlation between viability from the CyQuant Direct Cell assay and LAP concentration. Values represent $\bar{X} \pm SD$ pooling the values from all UV exposure treatment groups for each tested LAP concentration. Dotted lines represent the 95% confidence band.

decreasing viability with increasing LAP concentration in the investigated region.

C. Increasing cross-linking duration yields extracts with lower photocatalytic potential

Photocatalytic activity toward the oxidation of NADH to NAD^+ was measured for LAP (Fig. 4) and the formulation extracts (Fig. 5). Solutions of LAP (0.01 mg/ml) exposed to 7 mW/cm^2 of visible (>400 nm) light did not have any measurable photocatalytic effect but exhibited a 1011 ± 210 mol/(min g) catalytic rate when exposed to 5.5 mW/cm^2 UV-A (350–400 nm) light.

Photocatalytic properties of all extracts exposed to UV-A light were generally within an order of magnitude of the photocatalytic rate of 0.01 mg/ml LAP. Increasing LAP concentration in the GelMA photopolymer formulation was associated with increasing photocatalytic activity of the extract. Conversely, increasing UV exposure during cross-linking was associated with a decrease in the extract's photocatalytic activity.

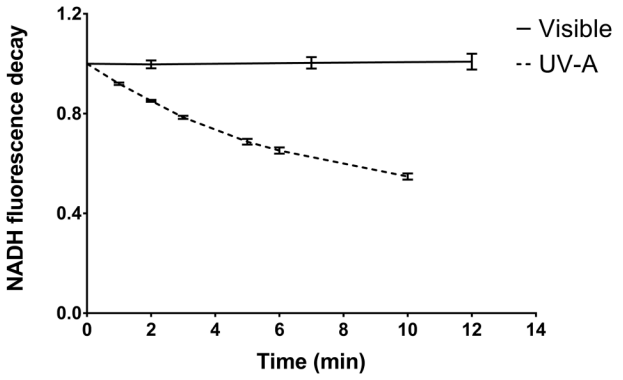

FIG. 4. Ratio of NADH fluorescence intensity of NADH photocatalyzed to NAD^+ in the presence of 0.01 mg/ml LAP to NADH alone. Samples were exposed to visible (>400 nm; 7 mW/cm^2) or UV-A (350–400 nm; 5.5 mW/cm^2) light, and the fluorescence intensity at 340 nm excitation and 460 nm emission wavelengths was determined at each timepoint. The derivative of the curve at t = 0 was used to calculate the photocatalytic activity toward NADH oxidation. Values represent $\bar{X} \pm SD$ of n = 6 technical replicates.

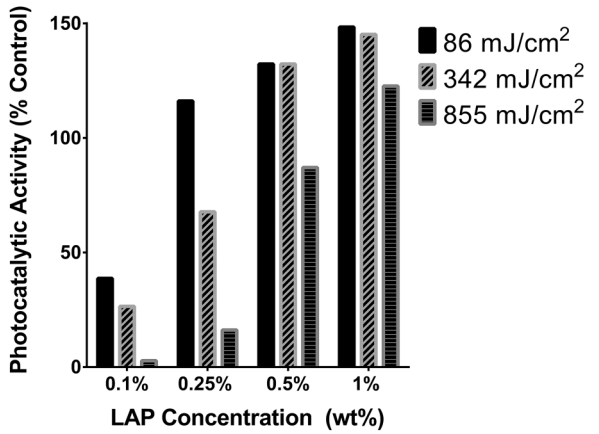

FIG. 5. Photocatalytic activity of GelMA-LAP extracts normalized to the activity of 0.01 mg/ml LAP in water. Values represent averages of n = 3 independent experimental replicates.

D. GelMA reaches stable elastic moduli after 120 s UV-A exposure

Elastic moduli (E_{IT}) were determined using nanoindentation from an average of seven measurements performed on a representative GelMA chip from each of the 12 formulations (Fig. 6). Nanoindentation can be applied to wide array of material types and can precisely measure elastic modulus and hardness without having to measure the postindentation impression.[26] Nanoindentation is also widely applied to biological materials with larger indenters to avoid piercing the sample.[27] In this study, use of a 500 μm spherical tip was appropriate for softer substrates such as GelMA and avoids edge stresses associated with flat-tip geometries. Measurement at multiple locations on the GelMA surfaces reduced error from time-dependent changes in the material and made measurements representative of the entire surface rather than that of a single point. Within each tested LAP concentration, E_{IT} increased between the 86 and 342 mJ/cm^2 UV-A exposures. However, for all samples except for the 0.1% w/w LAP concentration group, the elastic moduli between the 342 and 855 mJ/cm^2 exposures were similar. A slight downward trend in elastic modulus was noted with increasing LAP concentration with the 0.25%, 0.5%, and

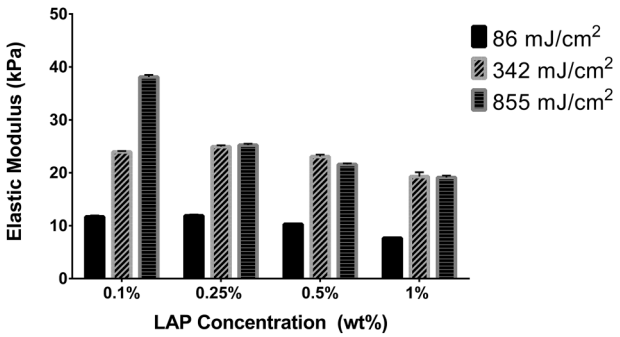

FIG. 6. Elastic moduli of 10% GelMA chips determined via nanoindentation. Values represent $\bar{X} \pm SD$ of n = 7 measurements at different locations on the GelMA chips.

1.0% LAP gels at 25.2, 23.1, and 19.1 kPa, respectively, for the 855 mJ/cm^2 exposure and 11.9, 10.3, and 7.6 kPa for the 86 mJ/cm^2 exposure.

IV. DISCUSSION

When considering materials for tissue engineering applications, hydrogel parameters such as mechanical properties, solidification mechanism, and cytocompatibility must be understood. Photosensitive polymers are attractive for tissue engineering because of their tunable mechanical properties and their ability to be precisely patterned. The benefits of photopolymers in tissue engineering are balanced by the reduced cytocompatibility stemming from the presence of ROS-generating photoinitiators and monomers involved in the cross-linking process. For these reasons, this study evaluated a common GelMA hydrogel with LAP photoinitiator by examining not only its cytocompatibility and mechanical properties, but also its photosensitizing potential. Fabrication of tissue engineering constructs proceeds in one of two paradigms: fabrication of an acellular scaffold followed by cell seeding or direct fabrication with cells *in situ*. In the former case, cells are isolated from the cross-linking process and could be further protected by aging the scaffold in solvents to leach out toxic substances. In the latter case, cells would be exposed to potential toxicant agents in any, or combination of, four phases: (1) chemical exposure when suspended within the unreacted photopolymer, (2) light exposure in the presence of photoinitiator, (3) exposure to by-products of the cross-linking reaction, and (4) exposure to degradation products during long-term culture. In this study, hRPTECs were exposed to GelMA photopolymer extracts to assess cytotoxic responses in phase 3 and is an experimental model that is more relevant to assess the effects of freshly implanted GelMA on surrounding tissues.

Alamar Blue and CyQuant were performed as viability assays but demonstrated contrasting results. The metabolism-based Alamar Blue assay showed no reduction in cell viability for any extract, but the CyQuant assay showed reduced viability correlated with the LAP concentration in the photopolymer formulation. This unexpected outcome might be related to the difference in the mechanistic basis of each assay. Since hRPTEC metabolism is unaffected, one possible explanation is injury of the cell membrane allowing the fluorescence suppression dye to enter. Cells with damaged cell membranes are generally necrotic, which is the assumption of the CyQuant Direct Cell assay and other assays that operate on a similar membrane-damage mechanism, such as Neutral Red or Trypan Blue. However, membrane permeabilization without significant loss of viability is possible and is sometimes sought after for applications like drug delivery. For example, ultrasound was used to deliver 70 kDa dextran into KHT-C murine fibrosarcoma cells; viability above 90% was observed with successful permeabilization of approximately 20% of the cells.[28] Investigation of the effect of membrane properties on extracellular or intracellular ROS-induced cell death revealed viability on par with the control of MDA-MB-231 breast cancer cells permeabilized with 0.002% saponin.[29] The mechanism of phospholipid bi-layer poration due to lipid oxidation was also determined with model 1,2-dioleoyl-sn-glycero-3-phosphocholine vesicles with exposure to methylene blue and phenothiazinium photosensitizers.[30] It is possible that the differences in results observed for these two viability assays are due to membrane poration.

Oxidative stress due to ROS from photoinitiator is a major concern during bioprinting with photopolymers and LAP could cause membrane poration. This oxidative potential was measured by the photosensitization screening method that tracks the oxidation of NADH to NAD$^+$. Significant quantities of photocatalytic material remained in all extracts with the photocatalytic potential increasing with increasing LAP concentration in the gel that represents a possible mechanism of membrane poration. However, increasing UV exposure decreased the photocatalytic potential consistent with photobleaching and should have affected the CyQuant signal. One explanation is that the cells in this study were not exposed to light and extract simultaneously, so the photoactive by-products of cross-linking were not activated.

Elastic moduli of the gels exposed to 342 and 866 mJ/cm^2 365 nm light were comparable for formulations containing 0.25%, 0.5%, and 1.0% LAP. These data contradict other studies reporting increasing elastic modulus or storage modulus with increasing photoinitiator concentrations and UV exposures exceeding multiple minutes.[5] Notably, many of these studies used Irgacure 2959 as the photoinitiator that has lower sensitivity to 365 nm light. For example, Fairbanks *et al.* reported gelation points for polyethyleneglycol diacrylate (PEGda) photoinitiated with 2.2 mmol/l Irgacure 2959 or LAP (corresponding approximately to 0.05% w/w) and cross-linked with 10 mW/cm^2 365 nm light.[18] Irgacure 2959 required ten times the light exposure duration versus LAP with a gelation time of 212 s vs 20 s. In addition, 0.22 mmol/l LAP using 365 nm light and 2.2 mmol/l LAP using 405 nm light had comparable gelation times at 141 and 120 s, respectively. Since a gelation time on the order of several minutes was required using Irgacure 2959, it is possible that other studies that report increasing gel stiffness with increasing UV exposure could be examining the region where cross-linking is still taking place. Duchi *et al.* also reported that increasing LAP concentration in a GelMA and hyaluronic acid gel correlated with increased storage modulus in an *in situ* photorheometry study.[31] However, gels containing 0.05% and 0.1% LAP exposed to continuous 365 nm light asymptotically reached the same storage modulus. When investigating the effect of different light exposure times on 0.1% LAP gels, 10 s of 100 mW/cm^2 illumination asymptotically reached the same ultimate storage modulus as the continuously illuminated sample. This result was corroborated by another photorheology study investigating GelMA with Irgacure 2959 to develop an empirical model predicting storage modulus. Equilibrium storage moduli obtained during *in situ* UV illumination was precisely predicted by GelMA

concentration. UV light intensity and photoinitiator concentration were not found to precisely predict the final storage modulus but instead predicted the cross-linking rate; the total UV exposure energy was proportional to the square root of intensity and inversely proportional to the square root of photoinitiator concentration.[32]

In the current study, 10% GelMA chips were exposed to UV in vast excess of the gelation point and should be expected to be fully cross-linked although the elastic modulus for sample D1, 10% GelMA with 0.1% w/w LAP and exposed to 855 mJ/cm^2 UV-A light, was significantly higher than the modulus for other gels at the same UV exposure. Given that this sample contained the lowest photoinitiator concentration, the elastic modulus should be equal to or less than the modulus of the other samples at equivalent UV-A exposure. GelMA at a 10% w/w concentration tend to have elastic moduli around 10–25 kPa depending on gelatin origin and degree of methacrylation.[33–35] Considering all other investigated LAP concentrations yielded similar elastic moduli when fully cross-linked, the uncharacteristically high elastic modulus of 38 kPa for 10% GelMA, especially with the lowest investigated LAP concentration, is atypical of this material. GelMA containing all other investigated LAP concentrations was fully cross-linked by the 342 mJ/cm^2 exposure corresponding to 120 s. GelMA with LAP photoinitiator should reach predictable elastic moduli using shorter cross-linking times practical for bioprinting applications.

V. SUMMARY AND CONCLUSIONS

Viability measurements of hRPTEC differed depending on whether the assay measured metabolic activity or membrane integrity. These cells, exposed to GelMA extracts generated from chips containing 1% LAP, exhibited viability on par with the negative control when measured with the Alamar Blue assay but had 67% viability when measured with the CyQuant Direct Cell assay. A cell viability of <70% is considered the threshold for cytotoxic potential as described in an international standard for biocompatibility assessment.[23] Further investigation on whether this GelMA + LAP material causes membrane poration would help understand more precisely the potential adverse cell interactions. Increasing cross-linking duration decreases the photopolymer extract's photocatalytic potential without significantly affecting the final elastic modulus; exhaustive cross-linking should be performed on acellular gels. Based on the results of the current study, cross-linking at 405 nm instead of 370 nm would be greatly preferred for cell-laden constructs. The commercial availability and widespread use of GelMA and LAP in bioprinting is a testament to its cytocompatibility but bioprinted and cell-laden photocrosslinkable hydrogels have been slow to reach a marketable form. High cell viability has been reported in the literature for GelMA and LAP and is mirrored in this study except for the highest LAP concentration, which is beyond the typical concentration used in bioprinting. The focus of future studies should shift to tissue function in different tissue models.

DISCLAIMER

The findings and conclusions in this paper have not been formally disseminated by the Food and Drug Administration and should not be construed to represent any agency determination or policy. The mention of commercial products, their sources, or their use in connection with material reported herein is not to be construed as either an actual or implied endorsement of such products by Department of Health and Human Services.

ACKNOWLEDGMENTS

The project is funded by the National Institutes of Health (NIH) under Grant No. R21-Al117748. The authors acknowledge Anton Paar's Mihaela Dubisson, Brandon Frye, and Nate Newbury for technical expertise and instrumentation (Biointenter UNHT3 Bio).

[1]X. Zheng Shu, Y. Liu, F. S. Palumbo, Y. Luo, and G. D. Prestwich, Biomaterials **25**, 1339 (2004).
[2]J. Yeh, Y. Ling, J. M. Karp, J. Gantz, A. Chandawarkar, G. Eng, J. Blumling Iii, R. Langer, and A. Khademhosseini, Biomaterials **27**, 5391 (2006).
[3]K. S. Lim *et al.*, Biofabrication **10**, 034101 (2018).
[4]Z. Wang, H. Kumar, Z. Tian, X. Jin, J. F. Holzman, F. Menard, and K. Kim, ACS Appl. Mater. Interfaces **10**, 26859 (2018).
[5]I. Pepelanova, K. Kruppa, T. Scheper, and A. Lavrentieva, Bioengineering **5**, 55 (2018).
[6]C. McBeth, J. Lauer, M. Ottersbach, J. Campbell, A. Sharon, and A. F. Sauer-Budge, Biofabrication **9**, 015009 (2017).
[7]W. Liu *et al.*, Adv. Healthc. Mater. **6**, 1601451 (2017).
[8]S. R. Govindarajan, T. Jain, J.-W. Choi, A. Joy, I. Isayeva, and K. Vorvolakos, Polymer **152**, 9 (2018).
[9]Y. Lin, C. Gao, D. Gritsenko, R. Zhou, and J. Xu, Microfluid. Nanofluid. **22**, 97 (2018).
[10]S. Bertlein *et al.*, Adv. Mater. **29**, 1703404 (2017).
[11]H. W. Ooi, C. Mota, A. T. ten Cate, A. Calore, L. Moroni, and M. B. Baker, Biomacromolecules **19**, 3390 (2018).
[12]S. Zheng, M. Zlatin, P. R. Selvaganapathy, and M. A. Brook, Addit. Manuf. **24**, 86 (2018).
[13]A. I. Van Den Bulcke, B. Bogdanov, N. De Rooze, E. H. Schacht, M. Cornelissen, and H. Berghmans, Biomacromolecules **1**, 31 (2000).
[14]H. Shirahama, B. H. Lee, L. P. Tan, and N. J. Cho, Sci. Rep. **6**, 31036 (2016).
[15]C. G. Williams, A. N. Malik, T. K. Kim, P. N. Manson, and J. H. Elisseeff, Biomaterials **26**, 1211 (2005).
[16]I. Mironi-Harpaz, D. Y. Wang, S. Venkatraman, and D. Seliktar, Acta Biomater. **8**, 1838 (2012).
[17]H. Ikehata *et al.*, J. Invest. Dermatol. **133**, 1850 (2013).
[18]B. D. Fairbanks, M. P. Schwartz, C. N. Bowman, and K. S. Anseth, Biomaterials **30**, 6702 (2009).
[19]W. E. Severus, N. Kleindienst, F. Seemüller, S. Frangou, H. J. Möller, and W. Greil, Bipolar Disord. **10**, 231 (2008).
[20]J. Baird-Gunning, T. Lea-Henry, L. C. G. Hoegberg, S. Gosselin, and D. M. Roberts, J. Intensive Care Med. **32**, 249 (2016).
[21]D. Marples, S. Christensen, E. I. Christensen, P. D. Ottosen, and S. Nielsen, J. Clin. Invest. **95**, 1838 (1995).
[22]K. S. Hodgkins and H. W. Schnaper, Pediatr. Nephrol. **27**, 901 (2012).
[23]International Organization for Standardization, see: https://www.iso.org/standard/36406.html for "Biological Evaluation of Medical Devices (ISO Standard No. 10993:2009)."
[24]N. A. Lee, S. J. Kim, B. J. Park, H. M. Park, M. Yoon, B. H. Chung, and N. W. Song, Photochem. Photobiol. Sci. **10**, 1979 (2011).
[25]K. L. Johnson, *Contact Mechanics* (Cambridge University, Cambridge, 1985).
[26]W. C. Oliver and G. M. Pharr, J. Mater. Res. **7**, 1564 (2011).

[27]L. Qian and H. Zhao, Micromachines **9**, 654 (2018).
[28]R. Karshafian, P. D. Bevan, R. Williams, S. Samac, and P. N. Burns, Ultrasound Med. Biol. **35**, 847 (2009).
[29]H. R. Molavian, A. Goldman, C. J. Phipps, M. Kohandel, B. G. Wouters, S. Sengupta, and S. Sivaloganathan, Sci. Rep. **6**, 27439 (2016).
[30]I. O. L. Bacellar, M. S. Baptista, H. C. Junqueira, M. Wainwright, F. Thalmann, C. M. Marques, and A. P. Schroder, Biochim. Biophys. Acta Biomembranes **1860**, 2366 (2018).
[31]S. Duchi *et al.*, Sci. Rep. **7**, 5837 (2017).
[32]C. O'Connell *et al.*, Soft Matter **14**, 2142 (2018).
[33]G. Eng, B. W. Lee, H. Parsa, C. D. Chin, J. Schneider, G. Linkov, S. K. Sia, and G. Vunjak-Novakovic, Proc. Natl. Acad. Sci. U.S.A. **110**, 4551 (2013).
[34]Z. Wang, Z. Tian, F. Menard, and K. Kim, Biofabrication **9**, 044101 (2017).
[35]X. Zhao *et al.*, Adv. Healthc. Mater. **5**, 108 (2016).